HAL open science

Phonons and Adsorption-Induced Deformations in ZIFs: Is It Really a Gate Opening?

Filip Formalik, Bartosz Mazur, Michael Fischer, Lucyna Firlej, Bogdan Kuchta

▶ **To cite this version:**

Filip Formalik, Bartosz Mazur, Michael Fischer, Lucyna Firlej, Bogdan Kuchta. Phonons and Adsorption-Induced Deformations in ZIFs: Is It Really a Gate Opening?. Journal of Physical Chemistry C, 2021, 125 (14), pp.7999-8005. 10.1021/acs.jpcc.1c01342 . hal-03226590

HAL Id: hal-03226590

https://amu.hal.science/hal-03226590

Submitted on 13 Jun 2022

HAL is a multi-disciplinary open access archive for the deposit and dissemination of scientific research documents, whether they are published or not. The documents may come from teaching and research institutions in France or abroad, or from public or private research centers.

L'archive ouverte pluridisciplinaire **HAL**, est destinée au dépôt et à la diffusion de documents scientifiques de niveau recherche, publiés ou non, émanant des établissements d'enseignement et de recherche français ou étrangers, des laboratoires publics ou privés.

Distributed under a Creative Commons Attribution 4.0 International License

THE JOURNAL OF PHYSICAL CHEMISTRY C
A JOURNAL OF THE AMERICAN CHEMICAL SOCIETY

pubs.acs.org/JPCC

Article

Phonons and Adsorption-Induced Deformations in ZIFs: Is It Really a Gate Opening?

Filip Formalik,* Bartosz Mazur, Michael Fischer, Lucyna Firlej, and Bogdan Kuchta

Cite This: *J. Phys. Chem. C* 2021, 125, 7999−8005

Read Online

ACCESS | Metrics & More | Article Recommendations | Supporting Information

ABSTRACT: We report a microscopic model of the phonon-adsorption correlations in flexible metal−organic framework materials. We analyze the mechanism of the gate opening deformation using the notion of coupled phonon- and adsorption-induced structural transformation. Using the ZIF-8 structure as an example, we perform an analysis of transformation-related, low-frequency phonon modes of the framework. On the basis of structure-related quantities such as pore limiting diameter, void fraction, and adsorption uptake, we determine the conditions which lead to the gate opening transformation in ZIF-8. Energetic landscape of the deformation process is analyzed using grand thermodynamic potential of adsorption. We generalize our conclusions to other flexible ZIF structures with the same topology.

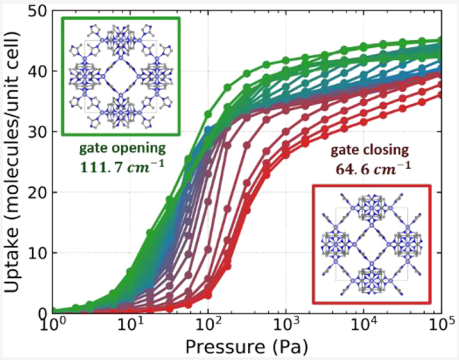

INTRODUCTION

Metal−organic frameworks (MOFs)[1] are crystalline, hybrid (organic−inorganic) nanoporous structures with tunable architecture. They are potentially applicable in many fields of chemistry and chemical engineering, such as gas capture, separation, catalysis, sensing, and many others.[2] A subgroup of MOFs, flexible MOFs, are frameworks which undergo a variety of structural deformations induced by different external stimuli such as pressure, temperature, electric field, and adsorption.[3] To explain the mechanism of adsorption-induced transformations, the phonon-driven deformation approaches have been explored;[4−6] nevertheless, despite many numerical and experimental works devoted to flexible MOFs, a comprehensive, generalized model of the microscopic mechanism of MOFs' deformations is still missing, mainly due to a variety of origins of the observed phenomena (rotation or buckling of the linkers,[7−10] sublattice displacement,[11] change of the angle between linkers,[12] and so forth).

ZIF-8, a sodalite (SOD) topology MOF built of Zn cations interconnected by imidazole linkers (Figure 1, center), undergoes a transformation usually referred to as "gate opening", involving a rotation of linkers which enlarges (or diminishes) the pore aperture.[10] This naturally impacts the adsorption-related properties, as the pore aperture (the gate) defines the ability of guest molecules to diffuse through the pores of the framework. In ZIF-8, the gate opening was previously reported to occur under high hydrostatic pressure[13−15] and was related to the adsorption of N_2.[10] However, the discrimination as to whether the step-on isotherm of nitrogen adsorption in ZIF-8 is caused by gate opening (linker reorientation) or by reorganization of the

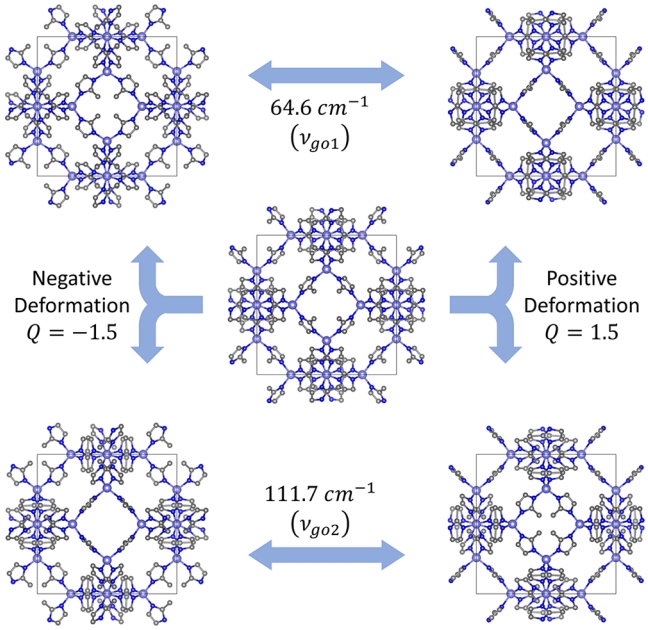

Figure 1. Structure of ZIF-8 (center). Structures deformed along (top) ν_{go1} and (bottom) ν_{go2} modes for negative and positive deformations (see the text for full explanation).

Received: February 13, 2021
Revised: March 19, 2021
Published: April 1, 2021

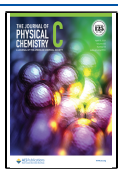

Downloaded via UNIV MONTPELLIER on June 13, 2022 at 15:46:08 (UTC).
See https://pubs.acs.org/sharingguidelines for options on how to legitimately share published articles.

ACS Publications
© 2021 The Authors. Published by American Chemical Society

https://doi.org/10.1021/acs.jpcc.1c01342
J. Phys. Chem. C 2021, 125, 7999−8005

adsorbate within the pore into a more densely packed configuration without adsorbent transformation was never achieved.[9,10] Most of the current theoretical models assume that the step present on the adsorption isotherm is associated with deformation of the host framework, defined by the frozen, low energy (frequency) phonons corresponding to linker-rotation-like vibrations.[4−6,16] Here, we analyze these phonons and discuss their role in the transformation occurring in ZIF-type MOFs.

In this work, we applied phonon formalism, density functional theory (DFT), and Grand Canonical Monte Carlo (GCMC) adsorption calculations to revisit the mechanism of the structural transformations in ZIF-type MOFs with SOD topology. We performed DFT calculations of low-frequency phonons and analyzed their potential contribution to the gate opening mechanism. For the first time, analysis of phonon-driven deformations of ZIFs was combined with quantities describing adsorption process such as pore limiting diameter (PLD) and void fraction (VF), explicit adsorption simulations, and grand thermodynamic potential of adsorption. This accounts for both phenomena in one model.

■ COMPUTATIONAL METHODS AND MODELS

Preparation of Phonon-Deformed Structures. In this work, we analyze structures which are derived from a DFT-optimized unit cell, where atoms are displaced according to deformation vectors $\mathbf{u}(i)$ related to particular phonon modes. These vectors are derived from polarization vectors $\mathbf{e}_\alpha$ (α is Cartesian coordinate) being eigenvectors of a 3D eigenvalue problem[17]

$$\omega^2(q)\mathbf{e}_\alpha = D(q)\mathbf{e}_\alpha \tag{1}$$

where $\omega(q)$ is the frequency of a mode at given q-point and $D(q)$ is the dynamical matrix. The deformation vector represents the instantaneous position of atom corresponding to a particular phonon

$$\mathbf{u}_\alpha = \frac{1}{\sqrt{m_i}} e_\alpha Q e^{\mathrm{iqR}} \tag{2}$$

where m_i is the mass of ith atom, Q is the amplitude of mode (scale of the eigenvector used to create deformed structure; we refer to it as deformation parameter,) and $e^{iq\mathrm{R}}$ is the plane wave which introduces the spatial dependence. Since we consider only phonons from the Γ-point of the Brillouin zone (for conventional, cubic cell $q = 0$), then the last term in eq 2 is equal to unity, and the deformation vector can be rewritten as

$$\mathbf{u}_\alpha = \frac{1}{\sqrt{m_i}} \mathbf{e}_\alpha Q \tag{3}$$

In this paper, the eigenvectors $\mathbf{e}_\alpha$ are extracted from VASP output file (OUTCAR) and deformed structures are prepared with our in-house python script.[18] The deformation parameter Q was varied from −1.5 to 1.5 [in units of Å·amu$^{1/2}$] with step of 0.1. The value $Q = 0$ corresponds to an undistorted (optimized) ZIF-8 structure, whereas for the limiting value $Q = 1.5$ we observe full opening of the gates in a previously reported gate opening mode[4−6] (with linkers in a four-member ring arranged in parallel to each other).

DFT Calculations. All phonon calculations have been performed on optimized structures for which the internal energy was found to be minimal. The structure optimization was performed using the VASP package and PAW method.[19−21] As previously reported,[22] long-range interactions were taken into account using Grimme D3(BJ) correction[23] to PBE density functional.[24] The convergence criteria were set to 10^{-6} eV for electronic degrees of freedom and to 10^{-4} eV/Å for ionic. Energy cutoff was set to 900 eV. Only one (Γ) k-point was considered due to large conventional unit cell of ZIF structures. Optimization was performed without symmetry constraint; the final symmetries of the optimized frameworks are listed in the Table S1. Frequencies are calculated using the finite displacement method with six displacements for each atom ($\pm\Delta x$, $\pm\Delta y$, $\pm\Delta z$, where each displacement was set to 0.01 Å), also considering only Γ-point (sufficiently large unit cell).

GCMC Calculations. GCMC simulations of the adsorption were performed using RASPA software.[25] Structures of the frameworks were taken from DFT calculations. To describe interactions in our system we used Lennard-Jones potential (6-12) parametrized according to UFF+ force field[26] for framework atoms and TraPPE[27] for N_2 molecules. UFF+ is based on UFF force field where ε parameters of LJ potential are divided by the factor of 1.69. Cross parameters were obtained with Lorentz−Berthelot mixing rules. Charges of framework atoms are calculated with eQeq[28] (method implemented in RASPA), as suggested in the benchmarking article by Sladekova et al.[29] Charges for N_2 molecule were taken from TraPPE force field. Spherical cutoff for LJ potential was set to 14 Å at which specific interactions were truncated (not shifted), and all interactions beyond this distance were calculated within mean-field approach (i.e., tail-correction was applied).

PLD and VF were calculated using algorithms available in the ZEO++ software.[30] All atomic structures and accessible surfaces were visualized in VESTA[31] and iRASPA[32] software, respectively. Absolute change of PLD and VF is defined as

$$\Delta X = X(\text{distorted structure}) - X(\text{undistorted structure}) \tag{4}$$

where X is considered parameter.

Accessible Surface. Accessible surfaces were calculated using iRASPA software[32] with nitrogen as a probe molecule. This surface is an isosurface where energy of interactions between probe and framework is equal to 0 ($r = \sigma_{\mathrm{LJ}}$). Practically, it means that the volume inside the pore corresponds only to the positions of the center of mass of adsorbed molecules. Hence, even a very thin channel which connects the neighboring pores indicates the possibility of gas diffusion in the framework.

Potential of Adsorption. Grand thermodynamic potential[33] for adsorbed phases is given as

$$\Omega_{\mathrm{ads}}(p, Q, T) = -RT\int_0^p \frac{N(p, Q, T)}{p}\,\mathrm{d}p, \tag{5}$$

where $N(p,Q,T)$ is the adsorption isotherm calculated for a unit cell deformed with deformation parameter Q and temperature T.

■ RESULTS AND DISCUSSION

Analysis of the DFT-derived phonon modes and their polarization vectors leads us to the conclusion that the low-frequency range of the vibrational spectra in ZIF-8 is totally dominated by modes related to linker rotations. The modes are divided into two groups, symmetric and asymmetric (for the

https://doi.org/10.1021/acs.jpcc.1c01342
J. Phys. Chem. C 2021, 125, 7999−8005

Table 1. Frequencies of the Modes Related to Imidazole Linker Rotation in ZIF-8[a]

	Frequency (cm^{-1})										
asymmetric linker rotation	102.3 (*T*)[b]	102.3 (*T*)[b]	99.9 (*T*)	98.7 (*T*)	94.1 (*T*)	84.9 (*T*)	81.9 (*T*)	70.7 (*T*)	69.1 (*T*)	68.0 (*T*)	58.8 (*T*)
symmetric linker rotation	**111.7**	103.8 (*D*)	87.0 (*D*)	77.0	67.9 (*D*)	**64.6**	55.8 (*D*)				

[a]Bold numbers represent ν_{go1} and ν_{go2} modes, described in detail in the text. *D* and *T* letters denotes modes which are doubly or triply degenerated modes, respectively. [b]Two different modes with similar frequencies.

distinction consult refs 4 and 34), and their frequencies are listed in Table 1. Visualization of all modes are available in SI.

We focus our analysis on two important modes occurring at 64.6 and 111.7 cm^{-1}. The mode at frequency 64.6 cm^{-1} (we called it ν_{go1} mode, Figure 1, top) was previously considered to be the most important in the gate-opening transformation[4−6] and for $Q = 1.5$ this mode changes the angle between linkers in the four-member ring by around 24°, leading to an essentially parallel orientation of the linkers. However, to the best of our knowledge no explicit relation between the deformation caused by the mode and its impact on the experimental adsorption isotherm was ever established. To get better insight into this aspect, we analyzed two structural parameters sensitive to the phonon deformations and, at the same time, affecting adsorption properties of a given structure: PLD, the diameter of the smallest pore aperture, and VF, the fraction of an empty space in volume of porous material. Both parameters were calculated for stable configuration of ZIF-8 (with geometry optimized at $T = 0$ K), and for hypothetical structures deformed along the deformation vectors u_α of few modes from low-frequency regime. The effect of deformation for selected modes and $Q = \pm 1.5$ is shown on Figure 1. We follow the convention adopted in the literature,[4,6] and call the deformations leading to the increase of the access to the pore a positive deformation.

Figure 2 shows the dependence of PLD and VF on the deformation parameter *Q*. Out of all modes listed in Table 1, the four modes impacting PLD and VF in the most significant way are shown here. Surprisingly, deformation related to the ν_{go1} mode causes a decrease of both parameters by 30% and 24% respectively. In consequence, the pore access is blocked, and the pore volume is decreased; consequently, the deformation rather should be called a "gate closing" deformation. The mode at frequency 103.8 cm^{-1} is doubly degenerated, however, as the deformations related to this mode exceeds by far harmonic region and nonzero deformation removes degeneracy, the corresponding VF and PLD are slightly different.

To visualize this transformation better, Figure 3 shows the surface accessible for adsorption in undistorted and distorted ZIF-8 structures. In undistorted structure, neighboring pores are connected by narrow apertures (formed by six Zn atoms connected by imidazole linkers, six-member ring), and therefore the diffusion of the gas through the system is possible. In the structure distorted according to ν_{go1} mode, these apertures disappear. It is a consequence of the blocking of six-member ring gates by hydrogen atoms from methyl groups attached to rotated linkers. As deformation progresses, for $Q \geq 1$ the PLD (Figure 2) decreases indicating that the gate is closing. A similar process is observed for the mode with frequency 76.95 cm^{-1} at even smaller deformation parameter $Q \geq 0.5$.

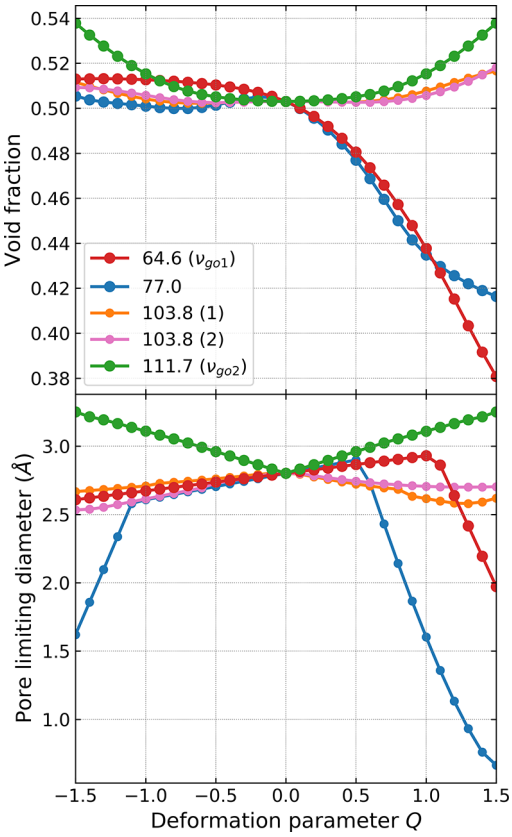

Figure 2. Void fraction (top) and pore limiting diameter (bottom) for structures deformed along selected symmetric gate-opening-related modes in ZIF-8 phonon spectrum. The mode at 103.8 cm^{-1} is doubly degenerated.

The mode with the frequency of 111.7 cm^{-1} (we call it ν_{go2} mode, see Figure 1) also involves linker rotation but has totally the opposite effect on PLD and VF parameters as compared to ν_{go1} mode. It is symmetric with respect to the negative and positive deformation and causes a constant, monotonic increase of PLD and VF as the deformation progresses (by 16% and 7%, respectively, for $Q = 1.5$, Figure 2). Consequently, both negative and positive deformations are in fact the same (graphical explanation provided in Figure S2). The increase of the gate diameter and subsequent variation of geometry of surface accessible for adsorption in the vicinity of the pore apertures (Figure 3, right panel) increases the probability of the guest molecules to diffuse between the neighboring pores. Therefore, ν_{go2} mode appears as a precursor of adsorption-induced gate opening deformation.

To analyze the explicit correlation between the deformation and adsorption, we performed simulations of nitrogen adsorption (at $T = 77$ K in undistorted ZIF-8 structure and in structures distorted according to ν_{go1} and ν_{go2} modes. Several simulation unit cells were prepared for deformation

https://doi.org/10.1021/acs.jpcc.1c01342
J. Phys. Chem. C 2021, 125, 7999−8005

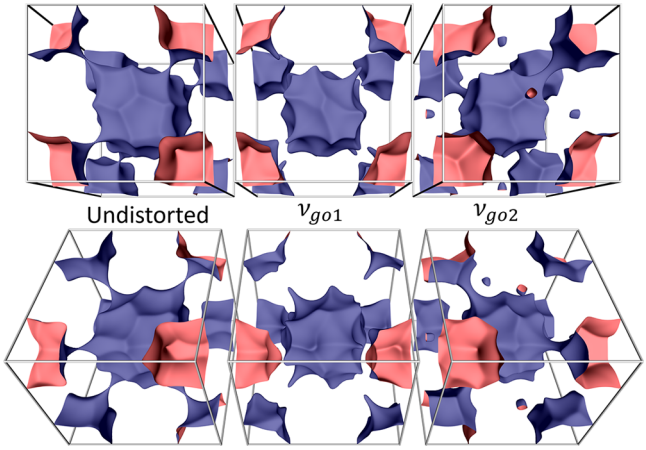

Figure 3. Surface accessible for adsorption in undistorted ZIF-8 structure and in the structures distorted along ν_{go1} and ν_{go2} modes for Q = 1.5. Nitrogen-like superatom has been used as a probing molecule. The cross sections of the unit cell along [100] (top) and [110] (bottom) are shown. Red and blue colors represent inner and outer surfaces, respectively.

parameter varying from 0 to 1.5. Figure 4 shows isotherms of adsorption for the outermost cases (Q = 1.5) compared to that

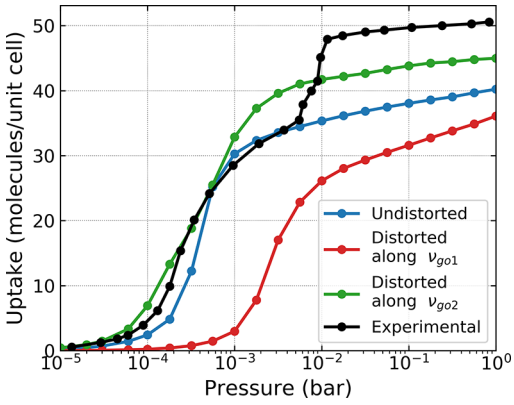

Figure 4. Simulated isotherms of nitrogen adsorption at 77 K in undistorted ZIF-8 and in frameworks deformed according to ν_{go1} and ν_{go2} modes for Q = 1.5. Experimental isotherm taken from ref 9.

calculated for undistorted structure (the isotherms for all intermediate structures ($0 < Q < 1.5$) for both modes are presented in the Figure S1) and an experimental isotherm.[9] For structures deformed along ν_{go1} mode, the adsorbed amount is smaller than in undistorted structure in the entire range of studied pressures. This observation suggests that ν_{go1}-type of deformation (i) decreases the strength of adsorption sites (at low pressures) and (ii) decreases the pore volume (at high pressure), as compared to the undistorted structure. In the structure deformed by ν_{go2} mode, the adsorbed amount is larger than in the undistorted structure (in the whole pressure range) although smaller than the one measured in the experiment.[9,10] Experimental adsorption isotherm (Figure 4, black) shows two steps: at the pressures of 0.005 and 0.009 bar. Experimentally, the first step was attributed to the gate-opening mechanism and the second to an expansion of the ZIF-8 framework (after structural deformation) upon adsorption.[9] The discrepancy between experiment and approach presented in this work can be related to several factors. First, in our calculations we use a ZIF-8 unit cell which, prior to phonon and adsorption calculations, was optimized at T = 0 K. Since ZIF-8 is a flexible material with positive volumetric thermal expansion coefficient,[35] we expect that at finite temperatures its unit cell and hence VF enlarges, causing an increase of the maximal gas uptake. Furthermore, in finite temperatures there are more types of vibrations occurring simultaneously, which can lead to a modification of the total capacity of the framework.

Figure 5 shows the change of grand thermodynamic potential of adsorption $\Delta\Omega_{ads}$ as a function of structure

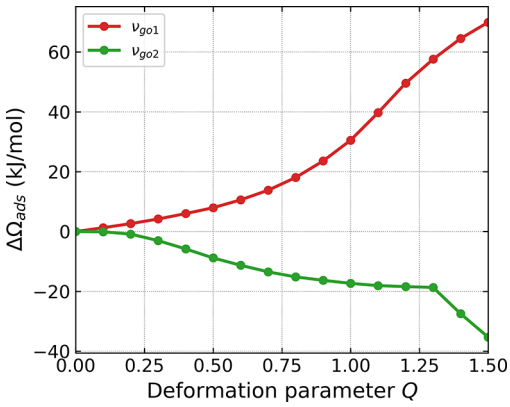

Figure 5. Grand thermodynamic potential of adsorption calculated for deformations related to two considered modes.

deformation ($0 < Q < 1.5$) according to ν_{go1} and ν_{go2} modes. $\Delta\Omega_{ads}$ provides insight into the system energy variation upon adsorption-induced deformation and was calculated from nitrogen adsorption isotherms (Figure S1; for theoretical details, see SI). For ν_{go1}-like deformation, $\Delta\Omega_{ads}$ rises monotonically as the deformation increases, reaching the value of almost 70 kJ/mol (of ZIF-8 conventional unit cell) for Q = 1.5 (fully open gate structure), hence this process requires the energy to be supplied to the system. On the contrary, in the case of ν_{go2}-like deformation $\Delta\Omega_{ads}$ progressively decreases, reaching the value of −35 kJ/mol for fully open gate conformation. As the energy required to deform ZIF-8 to a gate-opened phase, evaluated using ab initio molecular dynamics, is equal to approximately 15 kJ/mol,[36] we conclude that ν_{go2}-deformed structure is energetically stable in the presence of guest molecules adsorbed in the pore of ZIF-8, unlike the ν_{go1}-deformed structure. In other words, the ν_{go1}-like deformation may not be induced by adsorption.

To check whether chemical modification of ZIF-8 structure affects the mechanism of gate-opening transformation and related adsorption properties,[4,14,15,37] we extended our analysis to other ZIF materials which share the same sodalite topology and differ either in (i) functional group attached to imidazole linker (ZIF-90,[38] SALEM-2,[39] ZIF-8(Amino),[40] and ZIF-65[41]) or (ii) metal ion (BIF-3(Li),[42] BIF-3(Cu),[42] ZIF-67,[43] and CdIF-1[44]). The adopted selection protocol and a detailed description of frameworks is given in SI. Figure 6 (top) gives the values of frequencies of ν_{go1} and ν_{go2} modes in modified frameworks. As both modes exist in all studied structures, we conclude that they are characteristic for sodalite topology of the framework. The changes of PLD and VF in all distorted structures with respect to undistorted ones are given in Figure 6 (middle and bottom, respectively). For all frameworks with modified linkers, ν_{go1} and ν_{go2} related deformations result in a

https://doi.org/10.1021/acs.jpcc.1c01342
J. Phys. Chem. C 2021, 125, 7999−8005

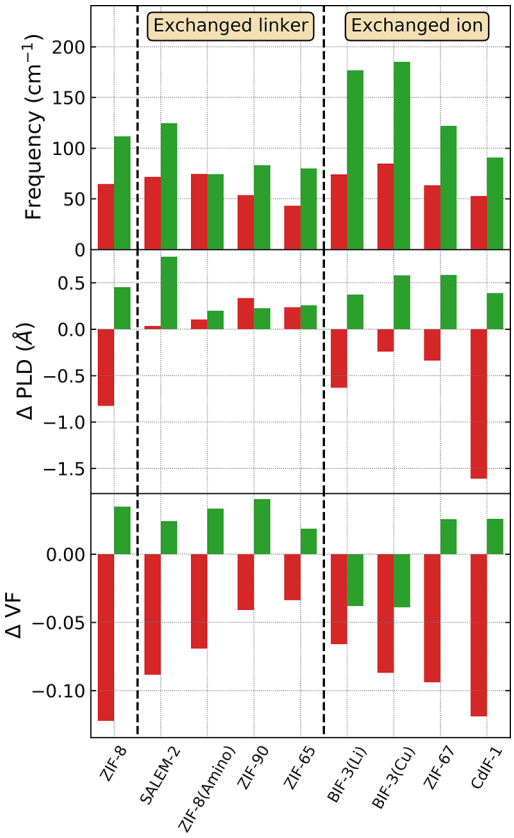

Figure 6. Frequencies of ν_{go1} and ν_{go2} modes (top), absolute change of pore limiting diameter ΔPLD (middle), and absolute change of void fraction ΔVF (bottom) in selected ZIF-type frameworks with SOD topology for deformation parameter Q = 1.5.

larger aperture of the pores (PLD changes are positive). It is caused by the planar nature of functional groups (or quasi-planar in the case of amino group) that are attached to substituted linkers and which do not block the 6-member ring aperture as observed in ZIF-8. Furthermore, the change of the chemical nature of the linkers affects the interactions between them, which may lead to the increase of gate opening effect. These results suggest that ZIF-type structures with SOD-type topology are more prone to undergo gate opening transformation initiated by ν_{go1} and or ν_{go2} lattice vibrations when the imidazole linker of the initial ZIF-8 structure is chemically modified. Two cation-modified frameworks (ZIF-67 and CdIF-1) show similar response to the ν_{go1} and ν_{go2} deformations as ZIF-8 (PLD is smaller or larger, respectively). For all systems deformed along ν_{go1} mode, the VF decreases, whereas for those deformed along ν_{go2} increases by several percent. An exception from this rule is observed for BIF-type materials of smaller (by 17%) unit cell volume than ZIF-8, resulting from shorter imidazole-B bonds (1.6 Å, to be compared to imidazole-Zn bond of 2.0 Å in ZIF-8).

CONCLUSIONS

In conclusion, our work shed new light on the question of the origin of the structural transformations in ZIF-type MOFs with sodalite topology. For the first time, analysis of phonon-driven deformations of ZIFs was combined with simulations of adsorption, to account for both phenomena at the same time. We have shown that low-frequency vibration mode at ν_{go1} = 64.6 cm^{-1}, which was previously associated with deformation causing an opening of the gates between pores actually causes gates' closing and disruption of the connections between neighboring pores. In consequence, the pore volume accessible for adsorption decreases in disaccord with the experimental observation of a rapid increase of the adsorbed amount at structure transformation. Moreover, in the low-frequency regime of ZIF-8 phonon spectrum we have identified another vibration mode at ν_{go2} = 111.7 cm^{-1}, consisting of a rotation of the imidazole linkers, which enlarges a six-member ring forming the pore aperture. The deformation of the structure according to this mode progressively increases both the diameter of the gate between the pores (gate opening deformation), and the fraction of structure volume accessible for adsorption. In consequence, the adsorption amount in the deforming structure is larger than in undeformed one which stays in agreement with the experimental results. On the basis of analysis of grand thermodynamic potential of adsorption, we prove that this type of the deformation is energetically favored. We also showed that the linker-rotation-type deformation of the framework is typical for imidazolate-based structures that show sodalite-topology but differ in the functional group attached to linker and metal cation. Since in solids there are many types of motions occurring simultaneously, in further studies the combination of two or more vibrational modes should also be considered as a source of static deformations of flexible structures.

Overall, the presented study confirms that the phonon analysis coupled with simulations of adsorption constitutes a useful tool to interpret adsorption-induced deformations and should be widely considered as a source of valuable microscopic information about the systems, complementary to experimental explorations.

ASSOCIATED CONTENT

Supporting Information

The Supporting Information is available free of charge at https://pubs.acs.org/doi/10.1021/acs.jpcc.1c01342.

Details on simulation methodology used in this work and description of the linker- and cation-modifications to ZIF-8 structure; animations of linker rotation modes; animation of the accessible surface construction (PDF)

AUTHOR INFORMATION

Corresponding Author

Filip Formalik − *Department of Micro, Nano, and Bioprocess Engineering, Faculty of Chemistry, Wroclaw University of Science and Technology, 50-370 Wroclaw, Poland; Department of Theoretical Physics, Faculty of Fundamental Problems of Technology, Wroclaw University of Science and Technology, 50-370 Wroclaw, Poland;* orcid.org/0000-0003-3981-3298; Email: filip.formalik@pwr.edu.pl

Authors

Bartosz Mazur − *Department of Micro, Nano, and Bioprocess Engineering, Faculty of Chemistry, Wroclaw University of Science and Technology, 50-370 Wroclaw, Poland*

Michael Fischer − *Crystallography Group, Faculty of Geosciences, University of Bremen, 28359 Bremen, Germany; MAPEX Center for Materials and Processes, University of Bremen, 28359 Bremen, Germany;* orcid.org/0000-0001-5133-1537

https://doi.org/10.1021/acs.jpcc.1c01342
J. Phys. Chem. C 2021, 125, 7999−8005

Lucyna Firlej − *Department of Micro, Nano, and Bioprocess Engineering, Faculty of Chemistry, Wroclaw University of Science and Technology, 50-370 Wroclaw, Poland; Charles Coulomb Laboratory, University of Montpellier, 34095 Montpellier, France;* orcid.org/0000-0002-8205-3522

Bogdan Kuchta − *Department of Micro, Nano, and Bioprocess Engineering, Faculty of Chemistry, Wroclaw University of Science and Technology, 50-370 Wroclaw, Poland; MADIREL, CNRS, Aix-Marseille University, 13397 Marseille, France;* orcid.org/0000-0002-8635-4154

Complete contact information is available at: https://pubs.acs.org/10.1021/acs.jpcc.1c01342

Notes

The authors declare no competing financial interest.

■ ACKNOWLEDGMENTS

F.F. was supported by the Polish National Science Centre (NCN, Grant ETIUDA No. 2018/28/T/ST4/00234). This research was supported in part by PL-Grid Infrastructure (DFT calculations). Calculations have been carried out using resources provided by Wroclaw Centre for Networking and Supercomputing, Grant 033 (GCMC calculations). M.F. acknowledges funding by the Deutsche Forschungsgemeinschaft (DFG, German Research Foundation), Project Number 389577027 (FI 1800/5-1). Internship of FF at University of Bremen was funded by the MAPEX Center for Materials and Processes, University of Bremen, through a Ph.D. Research Grant.

■ REFERENCES

(1) Zhou, H. C.; Long, J. R.; Yaghi, O. M. Introduction to Metal-Organic Frameworks. *Chem. Rev.* **2012**, *112* (2), 673−674.

(2) Furukawa, H.; Cordova, K. E.; O'Keeffe, M.; Yaghi, O. M. The Chemistry and Applications of Metal-Organic Frameworks. *Science.* **2013**, *341* (6149). DOI: 10.1126/science.1230444.

(3) Schneemann, A.; Bon, V.; Schwedler, I.; Senkovska, I.; Kaskel, S.; Fischer, R. A. Flexible Metal-Organic Frameworks. *Chem. Soc. Rev.* **2014**, *43* (16), 6062−6096.

(4) Formalik, F.; Fischer, M.; Rogacka, J.; Firlej, L.; Kuchta, B. Effect of Low Frequency Phonons on Structural Properties of ZIFs with SOD Topology. *Microporous Mesoporous Mater.* **2020**, *304*, 109132.

(5) Tan, N. Y.; Ruggiero, M. T.; Orellana-Tavra, C.; Tian, T.; Bond, A. D.; Korter, T. M.; Fairen-Jimenez, D.; Axel Zeitler, J. Investigation of the Terahertz Vibrational Modes of ZIF-8 and ZIF-90 with Terahertz Time-Domain Spectroscopy. *Chem. Commun.* **2015**, *51* (89), 16037−16040.

(6) Ryder, M. R.; Civalleri, B.; Bennett, T.; Henke, S.; Rudić, S.; Cinque, G.; Fernandez-Alonso, F.; Tan, J. C. Identifying the Role of Terahertz Vibrations in Metal-Organic Frameworks: From Gate-Opening Phenomenon to Shear-Driven Structural Destabilization. *Phys. Rev. Lett.* **2014**, *113* (21), 1−6.

(7) Evans, J. D.; Bocquet, L.; Coudert, F. X. Origins of Negative Gas Adsorption. *Chem.* **2016**, *1* (6), 873−886.

(8) Krause, S.; Bon, V.; Senkovska, I.; Stoeck, U.; Wallacher, D.; Többens, D. M.; Zander, S.; Pillai, R. S.; Maurin, G.; Coudert, F. X.; et al. A Pressure-Amplifying Framework Material with Negative Gas Adsorption Transitions. *Nature* **2016**, *532* (7599), 348−352.

(9) Ania, C. O.; García-Pérez, E.; Haro, M.; Gutiérrez-Sevillano, J. J.; Valdés-Solís, T.; Parra, J. B.; Calero, S. Understanding Gas-Induced Structural Deformation of ZIF-8. *J. Phys. Chem. Lett.* **2012**, *3* (9), 1159−1164.

(10) Fairen-Jimenez, D.; Moggach, S. A.; Wharmby, M. T.; Wright, P. A.; Parsons, S.; Düren, T. Opening the Gate: Framework Flexibility in ZIF-8 Explored by Experiments and Simulations. *J. Am. Chem. Soc.* **2011**, *133* (23), 8900−8902.

(11) Kitagawa, S.; Kitaura, R.; Noro, S. Functional Porous Coordination Polymers. *Angew. Chem., Int. Ed.* **2004**, *43* (18), 2334−2375.

(12) Llewellyn, P. L.; Maurin, G.; Devic, T.; Loera-Serna, S.; Rosenbach, N.; Serre, C.; Bourrelly, S.; Horcajada, P.; Filinchuk, Y.; Férey, G. Prediction of the Conditions for Breathing of Metal Organic Framework Materials Using a Combination of X-Ray Powder Diffraction, Microcalorimetry, and Molecular Simulation. *J. Am. Chem. Soc.* **2008**, *130* (38), 12808−12814.

(13) Moggach, S. A.; Bennett, T. D.; Cheetham, A. K. The Effect of Pressure on ZIF-8: Increasing Pore Size with Pressure and the Formation of a High-Pressure Phase at 1.47 GPa. *Angew. Chem., Int. Ed.* **2009**, *48* (38), 7087−7089.

(14) Hobday, C. L.; Bennett, T. D.; Fairen-Jimenez, D.; Graham, A. J.; Morrison, C. A.; Allan, D. R.; Düren, T.; Moggach, S. A. Tuning the Swing Effect by Chemical Functionalization of Zeolitic Imidazolate Frameworks. *J. Am. Chem. Soc.* **2018**, *140* (1), 382−387.

(15) Hobday, C. L.; Woodall, C. H.; Lennox, M. J.; Frost, M.; Kamenev, K.; Düren, T.; Morrison, C. A.; Moggach, S. A. Understanding the Adsorption Process in ZIF-8 Using High Pressure Crystallography and Computational Modelling. *Nat. Commun.* **2018**, *9* (1), 1−9.

(16) Zhang, W.; Maul, J.; Vulpe, D.; Moghadam, P. Z.; Fairen-Jimenez, D.; Mittleman, D. M.; Zeitler, J. A.; Erba, A.; Ruggiero, M. T. Probing the Mechanochemistry of Metal-Organic Frameworks with Low-Frequency Vibrational Spectroscopy. *J. Phys. Chem. C* **2018**, *122* (48), 27442−27450.

(17) Dove, M. T. *Introduction to Lattice Dynamics*; Cambridge University Press, 1993.

(18) *GitHub*. https://github.com/b-mazur/phonons (accessed: 12/15/2020).

(19) Kresse, G.; Furthmuller, J. Efficiency of Ab-Initio Total Energy Calculations for Metals and Semiconductors Using a Plane-Wave Basis Set. *Comput. Mater. Sci.* **1996**, *6*, 15−50.

(20) Kresse, G.; Furthmuller, J. Efficient Iterative Schemes for Ab Initio Total-Energy Calculations Using a Plane-Wave Basis Set. *Phys. Rev. B: Condens. Matter Mater. Phys.* **1996**, *54* (16), 11169−11186.

(21) Kresse, G.; Hafner, J. Ab Initio Molecular Dynamics for Liquid Metals. *Phys. Rev. B: Condens. Matter Mater. Phys.* **1993**, *47* (1), 558−561.

(22) Formalik, F.; Fischer, M.; Rogacka, J.; Firlej, L.; Kuchta, B. Benchmarking of GGA Density Functionals for Modeling Structures of Nanoporous, Rigid and Flexible MOFs. *J. Chem. Phys.* **2018**, *149* (6), 064110.

(23) Grimme, S.; Ehrlich, S.; Goerigk, L. Effect of the Damping Function in Dispersion Corrected Density Functional Theory. *J. Comput. Chem.* **2011**, *32*, 1456−1465.

(24) Perdew, J. P.; Burke, K.; Ernzerhof, M. Generalized Gradient Approximation Made Simple. *Phys. Rev. Lett.* **1996**, *77* (18), 3865−3868.

(25) Dubbeldam, D.; Calero, S.; Ellis, D. E.; Snurr, R. Q. RASPA: Molecular Simulation Software for Adsorption and Diffusion in Flexible Nanoporous Materials. *Mol. Simul.* **2016**, *42* (2), 81−101.

(26) Fairen-Jimenez, D.; Galvelis, R.; Torrisi, A.; Gellan, A. D.; Wharmby, M. T.; Wright, P. A.; Mellot-Draznieks, C.; Düren, T. Flexibility and Swing Effect on the Adsorption of Energy-Related Gases on ZIF-8: Combined Experimental and Simulation Study. *Dalt. Trans.* **2012**, *41* (35), 10752−10762.

(27) Potoff, J. J.; Siepmann, J. I. Vapor-Liquid Equilibria of Mixtures Containing Alkanes, Carbon Dioxide, and Nitrogen. *AIChE J.* **2001**, *47* (7), 1676−1682.

(28) Wilmer, C. E.; Kim, K. C.; Snurr, R. Q. An Extended Charge Equilibration Method. *J. Phys. Chem. Lett.* **2012**, *3* (17), 2506−2511.

(29) Sladekova, K.; Campbell, C.; Grant, C.; Fletcher, A. J.; Gomes, J. R. B.; Jorge, M. The Effect of Atomic Point Charges on Adsorption Isotherms of CO2 and Water in Metal Organic Frameworks. *Adsorption* **2019**. DOI: 10.1007/s10450-019-00187-2.

(30) Willems, T. F.; Rycroft, C. H.; Kazi, M.; Meza, J. C.; Haranczyk, M. Algorithms and Tools for High-Throughput Geometry-Based Analysis of Crystalline Porous Materials. *Microporous Mesoporous Mater.* **2012**, *149* (1), 134−141.
(31) Momma, K.; Izumi, F. VESTA 3 for Three-Dimensional Visualization of Crystal, Volumetric and Morphology Data. *J. Appl. Crystallogr.* **2011**, *44* (6), 1272−1276.
(32) Dubbeldam, D.; Calero, S.; Vlugt, T. J. H. IRASPA: GPU-Accelerated Visualization Software for Materials Scientists. *Mol. Simul.* **2018**, *44* (8), 653−676.
(33) Coudert, F. X.; Jeffroy, M.; Fuchs, A. H.; Boutin, A.; Mellot-Draznieks, C. Thermodynamics of Guest-Induced Structural Transitions in Hybrid Organic-Inorganic Frameworks. *J. Am. Chem. Soc.* **2008**, *130* (43), 14294−14302.
(34) Maul, J.; Ryder, M. R.; Ruggiero, M. T.; Erba, A. Pressure-Driven Mechanical Anisotropy and Destabilization in Zeolitic Imidazolate Frameworks. *Phys. Rev. B* **2019**, *99* (1), 1−7.
(35) Bouëssel Du Bourg, L.; Ortiz, A. U.; Boutin, A.; Coudert, F. X. Thermal and Mechanical Stability of Zeolitic Imidazolate Frameworks Polymorphs. *APL Mater.* **2014**, *2* (12). DOI: 10.1063/1.4904818.
(36) Coudert, F. X. Molecular Mechanism of Swing Effect in Zeolitic Imidazolate Framework ZIF-8: Continuous Deformation upon Adsorption. *ChemPhysChem* **2017**, 1−8.
(37) Fischer, M.; Bell, R. G. Interaction of Hydrogen and Carbon Dioxide with Sod-Type Zeolitic Imidazolate Frameworks: A Periodic DFT-D Study. *CrystEngComm* **2014**, *16* (10), 1934.
(38) Morris, W.; Doonan, C. J.; Furukawa, H.; Banerjee, R.; Yaghi, O. M. Crystals as Molecules: Postsynthesis Covalent Functionalization of Zeolitic Imidazolate Frameworks Crystals as Molecules: Postsynthesis Covalent Functionalization of Zeolitic Imidazolate Frameworks. *J. Am. Chem. Soc.* **2008**, *130*, 12626−12627.
(39) Karagiaridi, O.; Lalonde, M. B.; Bury, W.; Sarjeant, A. A.; Farha, O. K.; Hupp, J. T. Opening ZIF-8: A Catalytically Active Zeolitic Imidazolate Framework of Sodalite Topology with Unsubstituted Linkers. *J. Am. Chem. Soc.* **2012**, *134* (45), 18790−18796.
(40) Houndonougbo, Y.; Signer, C.; He, N.; Morris, W.; Furukawa, H.; Ray, K. G.; Olmsted, D. L.; Asta, M.; Laird, B. B.; Yaghi, O. M. A Combined Experimental-Computational Investigation of Methane Adsorption and Selectivity in a Series of Isoreticular Zeolitic Imidazolate Frameworks. *J. Phys. Chem. C* **2013**, *117* (20), 10326−10335.
(41) Tu, M.; Wiktor, C.; Rösler, C.; Fischer, R. A. Rapid Room Temperature Syntheses of Zeolitic-Imidazolate Framework (ZIF) Nanocrystals. *Chem. Commun.* **2014**, *50* (87), 13258−13260.
(42) Zhang, J.; Wu, T.; Zhou, C.; Chen, S.; Feng, P.; Bu, X. Zeolitic Boron Imidazolate Frameworks. *Angew. Chem., Int. Ed.* **2009**, *48* (14), 2542−2545.
(43) Banerjee, R.; Phan, A.; Wang, B.; Knobler, C.; Furukawa, H.; O'Keeffe, M.; Yaghi, O. M. High-Throughput Synthesis of Zeolitic Imidazolate Frameworks and Application to CO2 Capture. *Science* **2008**, *319*, 939−943.
(44) Tian, Y.-Q.; Yao, S.-Y.; Gu, D.; Cui, K.-H.; Guo, D.-W.; Zhang, G.; Chen, Z.-X.; Zhao, D.-Y. Cadmium Imidazolate Frameworks with Polymorphism, High Thermal Stability, and a Large Surface Area. *Chem. - Eur. J.* **2010**, *16* (4), 1137−1141.

https://doi.org/10.1021/acs.jpcc.1c01342
J. Phys. Chem. C 2021, 125, 7999−8005